# A Combined Theoretical and Experimental Research Project into the Aminolysis of β-Lactam Antibiotics: The Importance of Bifunctional Catalysis

Natalia Díaz,[a] Dimas Suárez,[a] Tomás L. Sordo,*[a] Rosa Méndez,[b] and Javier Martín Villacorta*[b]

**Keywords:** Aminolysis / Antibiotics / Density functional calculations / Kinetics / Lactams

This paper reports the results of experimental work on the aminolysis of penicillin (6-APA) and monobactam (aztreonam) antibiotics by propylamine or ethanolamine. In general, aztreonam is slightly more reactive than 6-APA, despite the common assumption that the amide bond should be less activated in monobactams. Intriguingly, when ethanolamine acts as the nucleophile, the corresponding rate law has a kinetic term proportional to $[RNH_2][RNH_3^+]$. To complement the experimental observations, the rate-determining free energy barriers in aqueous solution for various mechanistic pathways were computed by standard quantum chemical methodologies. From previous theoretical work it was assumed that the aminolysis of β-lactams proceeds through mechanisms in which either a water molecule or a second amine molecule may act as bifunctional catalysts, assisting proton transfer from the attacking amine molecule to the leaving amino group. The energy barriers as computed have moderate values (ca. 26–34 kcal·mol$^{-1}$) and reproduce most of the experimentally observed kinetic trends. Furthermore, the calculations predict that positively charged ethanolamine molecules can act as bifunctional catalysts as well, thus explaining the presence of the kinetic term proportional to $[RNH_2][RNH_3^+]$ in the rate law.



## Introduction

The major antigenic determinant of penicillin allergy detected by the immunological system is the penicilloyl group bound by an amide linkage to ε-amino groups of lysine residues in plasma proteins.[1,2] In addition, allergy skin tests for the determination of IgE antibodies to penicillins consist of the penicilloyl reagent resulting from aminolysis of the β-lactam ring by polylysine or Human Serum Albumin (HSA) carrier molecules.[3] In order to understand these biochemical processes in more detail, the aminolysis of β-lactam compounds has been extensively studied experimentally.[4−13]

For a series of primary monoamines, it has been found that the importance of the different reaction pathways resulting in the disappearance of the β-lactam compounds from aqueous amine solution depends on the p$K_a$, on the concentration of the amine and on pH. The experimentally observed pseudo-first order rate constant $k_{obs}$ is made up of several terms corresponding to the various reactive processes. This is expressed by the following Equation (1).

$$k_{obs} = k_{pH} + k_1[RNH_2] + k_2[RNH_2][RNH_2] + k_3[RNH_2][OH^-] \quad (1)$$

$k_{pH}$ is the first order rate constant for the hydrolysis reaction, which is normally less than 15% of $k_{obs}$ except under high pH conditions, in which alkaline hydrolysis becomes the most important process. The kinetic constants corresponding to uncatalysed ($k_1$) and amine-catalysed ($k_2$) aminolysis are the predominant terms when weakly basic amines react with β-lactams in the biologically relevant pH range from 6 to 8. For strongly basic amines, the amine-catalysed ($k_2$) and hydroxide-catalysed ($k_3$) processes contribute most to the aminolysis reaction, the $k_2$ term being more important through increasing amine concentration.

Kinetic experiments have provided a mechanistic insight into the different routes for aminolysis of β-lactams. Most importantly, the non-linear dependence of the rate of aminolysis ($k_{obs}-k_{pH}$) of benzylpenicillin and 6-β-aminopenicillanic acid upon hydroxide ion concentration has been interpreted in terms of the formation of a *zwitterionic* tetrahedral intermediate $\mathbf{T^{\pm}}$ by a stepwise mechanism (see Scheme 1).[11,3] In addition, the Brønsted β-values on the p$K_a$ of amines for uncatalysed ($k_1$) and amine-catalysed ($k_2$) aminolysis have values close to unity.[9,11] From conven-

[a] Departamento de Química Física y Analítica, Universidad de Oviedo,
C/ Julian Clavería, 8, 33006, Oviedo, Spain
Fax: (internat.) +34-985-103125
E-mail: tsordo@correo.uniovi.es
[b] Departamento de Química, Física y Expresión Gráfica, Universidad de León,
24071, León, Spain

Supporting information for this article is available on the WWW under http://www.eurjoc.org or from the author.

tional interpretation of the Brønsted plots,[14] it has been assumed that an amine molecule carries a unit positive charge at the relevant rate-determining Transition Structures (TSs) through the uncatalysed ($k_1$) and amine-catalysed ($k_2$) routes. This has been seen as consistent with the stepwise mechanism through *zwitterionic* intermediates $\mathbf{T}^{\pm}$ proposed both for the specific and for the general base-catalysed aminolysis of *all* types of β-lactam compounds.[11,13] General and specific base catalysis of the reaction would occur by proton transfer from $\mathbf{T}^{\pm}$ to a molecule of amine or a hydroxide anion, respectively, to form $\mathbf{T}^{-}$, which then would break down to products (see Scheme 1).[9]

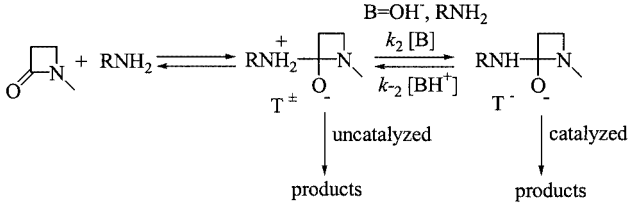


Scheme 1

Computational modelling predicts that the aminolysis of penicillin-like compounds in aqueous solution[15,16] can proceed through concerted mechanisms in which either a water molecule or a second amine molecule plays a crucial role as bifunctional catalyst in assisting proton transfer from the attacking amine molecule to the departing amino group (see Scheme 2). These theoretical results have also shown that a purely uncatalysed mechanism is not competitive with the water-assisted mechanism, which should therefore be the most important contributor to the $k_1$ term.[15] The computed rate-determining TSs are characterized by a nearly formed N(amine)−C(β-lactam) bond while the four-membered ring is hardly cleaved. These TSs have positive charges on the nucleophilic moiety (water-assisted process) or the catalytic amine molecule (amine-assisted route), thus explaining the reported positive Brønsted β values on $k_1$ and $k_2$ for the reaction between benzylpenicillin and a series of amines.[9]

Clearly, the theoretical description of the aminolysis reaction of β-lactams in Scheme 2 does not assign a crucial role to the zwitterions $\mathbf{T}^{\pm}$ proposed in Scheme 1. In fact, theoretical optimization of $\mathbf{T}^{\pm}$ structures in solution found them to be very unstable intermediate species with very short mean lifetimes before fragmentation into reactants even in strongly polar media.[17,18] Similarly, in a recent computer simulation of the model reaction $NH_3$ + HCOOH → $HCONH_2$ + $H_2O$ in aqueous solution,[19] it was discovered that although $\mathbf{T}^{\pm}$-like structures are formed at the beginning of the ammonolysis path, their lifetimes vary from 1 picosecond to only a few femtoseconds. In this scenario, the transition states sketched in Scheme 2 should be considered the most important *critical* structures, their geometries and energetics determining the mechanism of the aminolysis reaction of penicillins regardless of the actual lifetimes of the previous $\mathbf{T}^{\pm}$-like structures in solution.

In principle, the mechanistic routes assisted by either water or amine could well occur during the aminolysis of other bicyclic β-lactam compounds such as cephalosporins, penems, carbapenems, and the like. For monobactam antibiotics characterized by the presence of a *N*-sulfonate group, however, another competitive mechanism in aqueous solution might occur, according to quantum chemical calculations.[20] In this alternative mechanism, the *N*-$SO_3^-$ group plays an active kinetic role by assisting proton relay

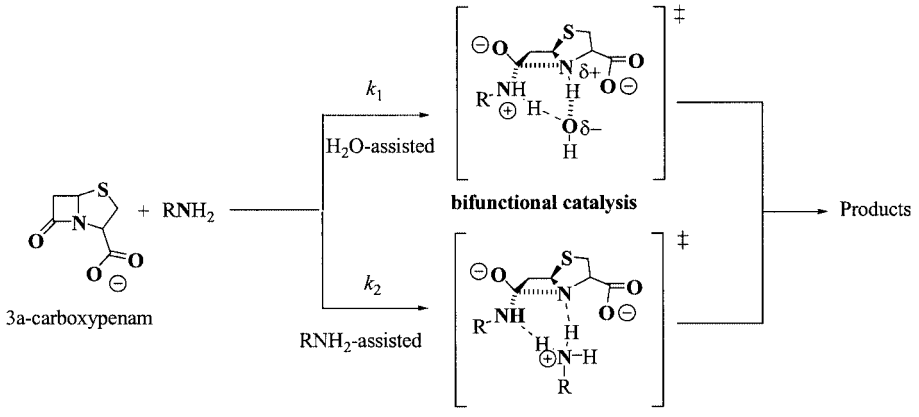


Scheme 2

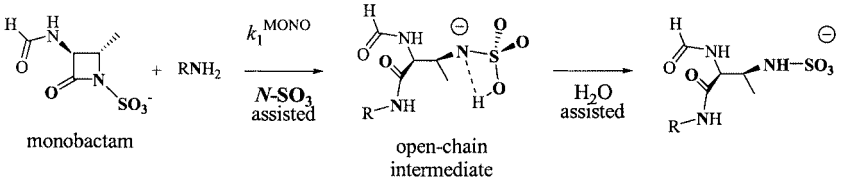


Scheme 3

  

from the attacking amine to the departing amino group and simultaneously favouring rupture of the β-lactam ring to give an open-chain intermediate (see Scheme 3).

This paper gives a report of a combined theoretical and experimental investigation of the aminolysis of penicillins and monobactams. Besides complementing previous work on the aminolysis of β-lactams, this article pursues a two-fold goal. On the one hand, it further demonstrates the ability of the theoretically proposed mechanisms to explain experimental data. A comparison is made of theoretically predicted and experimentally observed kinetic effects induced by the structure of the β-lactam (6-APA versus aztreonam; see Scheme 4) and the nature of the nucleophile. Emphasis is placed on the relative importance of the $k_1$ and $k_2$ kinetic terms in Equation (1), since these are presumably the most relevant processes for the biochemical activity of β-lactam antibiotics. On the other hand, kinetic parameters for the aminolysis of aztreonam (the first monobactam antibiotic to be marketed) are reported for the first time. Several competing mechanisms for the aminolysis of a monobactam model compound are theoretically characterized in order to estimate the actual kinetic impact of the $N$-$SO_3^-$ group. Overall, the results shed new light on the differences and similarities in structure and function of monocyclic and bicyclic β-lactam antibiotics. Moreover, these results are also of methodological interest, since they highlight the achievements and weaknesses of standard quantum chemical methodologies in helping interpretation of experimentally measured kinetic data for organic reactions in solution.

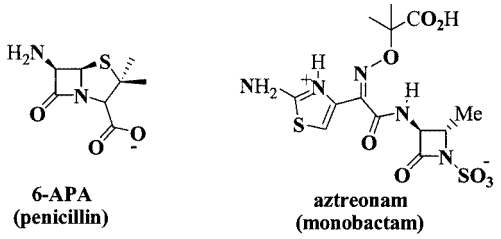


Scheme 4

## Results and Discussion

### Experimental Kinetics

As mentioned in the Introduction, the aminolysis of β-lactams studied in aqueous solution, in the presence of excesses of amines and at constant pH follows pseudo-first order kinetics. The pseudo-first order rate constant $k_{obs}$, obtained by a least-squares treatment from the slope of the semilogarithmic plots of the residual concentration versus time, is the sum of a first order hydrolysis rate, $k_{pH}$, and the first order rate constant depending on the concentration of amines, $k_{amine}$, so that once the value of $k_{pH}$ is known for each pH, $k_{amine}$ can be determined readily.

In this work, experiments were carried out in which $k_{obs}$ was experimentally determined as a function of the concentration of the amine, with the pH, ionic strength and temperature kept constant. The plots of $k_{obs}$ and $k_{amine}$ versus the total amine concentration ($[amine]_T$) for each pH showed an upward curvature at any pH value, which is indicative of a term second order in amine. The first order rate constant $k_{amine}$ apparently obeys the previously reported general relationship for penicillins and cephalosporins,[4−13] which can be rewritten in the following form by dividing Equation (1) by the total amine buffer concentration, where α is the fraction of the free base of the amine. Equation (2) predicts that plots of $k_{amine}/[amine]_T$ versus $[amine]_T$ will provide $k_2\,\alpha = k_{cat}$ as the slope and $\alpha(k_1 + k_3[OH^-]) = k_{int}$ as the intercept (see Figure 1).

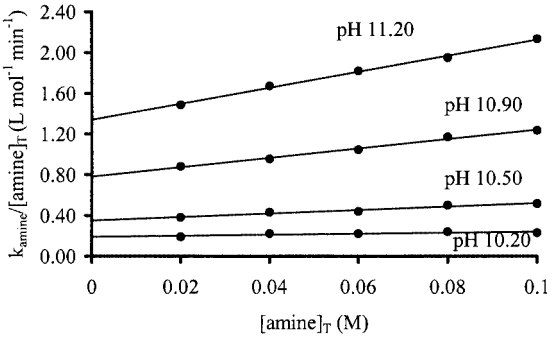


Figure 1. Second order rate constants for the reaction between propylamine and aztreonam in water at the indicated pH as a function of total amine concentration at 30.0 °C and 0.25 M ionic strength

$$\frac{k_{amine}}{[amine]_T} = k_1\alpha + k_2\alpha^2[amine]_T + k_3\alpha[OH^-] \quad (2)$$

On the other hand, plots of $k_{cat}/\alpha$ versus α gives straight lines, as illustrated in Figures 2 and 3 for the aminolysis of Aztreonam and 6-APA with propylamine and ethanolamine, respectively. The intercepts of these plots at $\alpha = 0$ and $\alpha = 1$ give the rate constants for any term in the rate law proportional to $[RNH_2][RNH_3^+]$ and $[RNH_2]^2$ respectively (i.e., $k_2$).

Plots of $k_{int}$ against α are non-linear and show upward curvature (not shown). This indicates that the hydroxide ion-catalysed reaction makes a significant contribution to the observed rate even in buffer solutions. A plot of $k_{int}/\alpha$

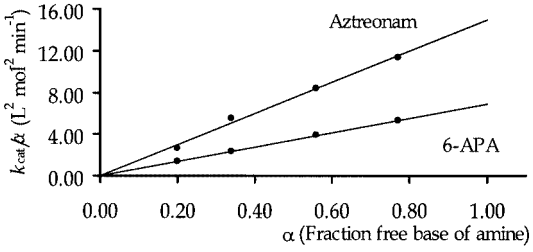


Figure 2. Plots of third order rate constants, $k_{cat}/\alpha$ (from the slopes of graphs as in Figure 1), versus the fraction of free base (α) of the buffer for the reaction between aztreonam or 6-APA and *propylamine* in water; the ordinate intercepts at $\alpha = 0$ and $\alpha = 1$ give the catalytic constants for the acidic and the basic species of the buffer

  

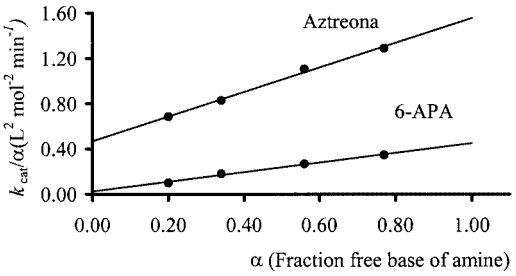


Figure 3. Plots of third order rate constants, $k_{cat}/\alpha$ (from the slopes of graphs as in Figure 1), versus the fraction of free base (α), of the buffer for the reactions between aztreonam or 6-APA and *ethanolamine* in water; the ordinate intercepts at α = 0 and α = 1 give the catalytic constants for the acidic and the basic species of the buffer

versus hydroxide ion concentration is linear and provide $k_3$ as the slope and $k_1$ as the intercept (see Figures 4 and 5).

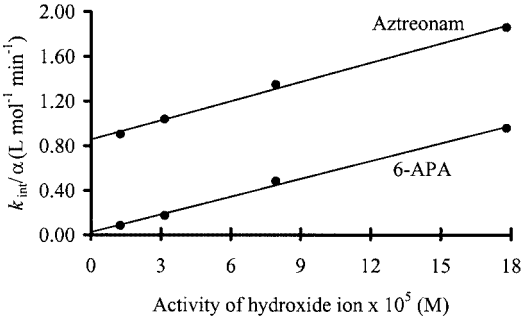


Figure 4. Plots of second order rate constant, $k_{int}/\alpha$ (from the intercepts of graphs as in Figure 1), versus the activity of hydroxide ion for the reactions between aztreonam or 6-APA and *propylamine* in water; the slope gives $k_3$ and the intercept $k_1$

The values of the $k_1$, $k_2$, and $k_3$ constants for the aminolysis processes of 6-APA and aztreonam with propylamine and ethanolamine are summarized in Table 1. The corresponding kinetic constants determined for benzylpenicillin in previous work[9] are also shown for comparison. Both 6-APA and benzylpenicillin exhibit similar reactivities against amine nucleophiles. On the other hand, the $k_1$, $k_2$, and $k_3$ constants for aztreonam are not far from those for the penicillins. However, a more detailed comparison between the kinetic data of 6-APA and aztreonam in reaction with propylamine indicates that aztreonam is more reactive, especially in the case of the $k_1$ route, by a factor of 34. This is in contrast with common assumptions that the amide bond should be more activated in penicillins than in monobactams, due to the greater pyramidalization of the endocyclic N atom in the bicyclic penicillins. On the other hand, the kinetic constants for ethanolamine as the attacking amine tend to be lower than those for propylamine except in the case of the $k_1$ route in reaction with 6-APA. This is usually interpreted in terms of the lower nucleophilicity and basic strength of the amino group of ethanolamine in relation to propylamine. Intriguingly, non-negligible terms were found in the rate law proportional to $[RNH_2][RNH_3^+]$ for ethanolamine in reaction either with aztreonam or with 6-APA. This result contrasts with previous reports on the aminolysis of benzylpenicillin,[9] in which only hydrazine presented a non-negligible $k_2$ term on $[RNH_2][RNH_3^+]$.

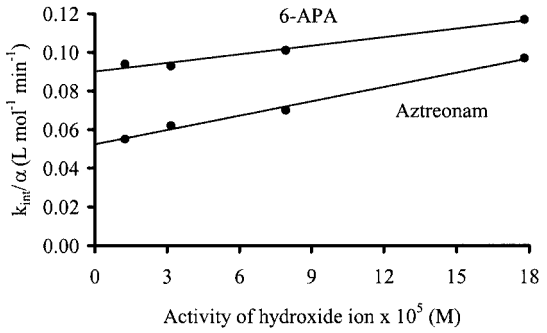


Figure 5. Plots of second order rate constant, $k_{int}/\alpha$ (from the intercepts of graphs as in Figure 1), versus the activity of hydroxide ion for the reactions between aztreonam or 6-APA and *ethanolamine* in water; the slope gives $k_3$ and the intercept $k_1$

### Theoretical Characterization of Transition Structures

To find out whether the theoretically proposed mechanism can account for the kinetic trends shown by the $k_1$ and $k_2$ values in Table 1, a series of TSs were characterized for the aminolysis of two model compounds (**APA** and **MONO**, see Scheme 5) in reaction with methylamine and ethanolamine. The model compounds **APA** and **MONO** mimic the nucleus of 6-APA and aztreonam, respectively. The 6-amino group of APA was simulated in its deprotonated (neutral) form, as the corresponding p$K_a$ in water

Table 1. Rate constants for the reactions of 6-APA, aztreonam, and benzylpenicillin with amine buffers at 30.0 °C and ionic strength 0.25 M

| β-Lactam | Amine | p$K_a$ | $k_1$ L·mol$^{-1}$·min$^{-1}$ | $k_2$[a] L$^2$·mol$^{-2}$·min$^{-1}$ | $k_2$[b] L$^2$·mol$^{-2}$·min$^{-1}$ | $k_3$ L$^2$·mol$^{-2}$·min$^{-1}$ |
|---|---|---|---|---|---|---|
| 6-APA | Propylamine | 10.79 | $2.50\cdot10^{-2}$ | 6.66 | ~ 0 | $5.34\cdot10^{3}$ |
| | Ethanolamine | 9.73 | $9.04\cdot10^{-2}$ | 0.455 | 0.0186 | $1.46\cdot10^{2}$ |
| Aztreonam | Propylamine | 10.79 | 0.851 | 15.24 | ~ 0 | $5.76\cdot10^{3}$ |
| | Ethanolamine | 9.73 | $5.18\cdot10^{-2}$ | 1.56 | 0.469 | $2.54\cdot10^{2}$ |
| Benzylpenicillin | Propylamine | 10.79 | $7.92\cdot10^{-2}$ | 63 | ~ 0 | $2.88\cdot10^{3}$ |
| (ref. [9]) | Ethanolamine | 9.73 | 0.336 | 4.65 | ~ 0 | $6.60\cdot10^{2}$ |

[a] For the kinetic term proportional to $[RNH_2]^2$ (see text for details). [b] For the kinetic term proportional to $[RNH_2][RNH_3^+]$ (see text for details).

  

has been reported to be only 4.9.[21] For computational economy, methylamine was used in the calculations instead of the propylamine used experimentally.

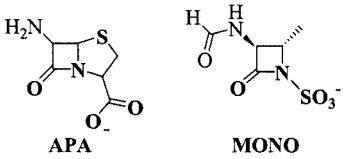


Scheme 5

Table 2 brings together the relative energy components ($\Delta E_{elec}$, $\Delta G_{solution}$, etc.) for the most important TSs relevant to the different reactive processes (i.e., APA + methylamine, APA + ethanolamine, MONO + methylamine, MONO + ethanolamine). The various energy terms in Table 2 are given with respect to separated reactants. In this respect, all the water-assisted processes are assumed to be bimolecular; that is, the β-lactam model compound reacts with a *dimer* formed between the ancillary water molecule and the nucleophilic amine.

Both the water- and the amine-catalysed mechanisms were considered for the aminolysis of **MONO** and **APA** with methylamine or ethanolamine. In addition, a third mechanism for the ethanolamine reaction was investigated, in which the hydroxy group of the amine plays an active kinetic role as a bifunctional catalyst. The electronic and geometrical features of this class of TSs have been thoroughly discussed in previous work on analogous systems[15,16] and so they will not be reviewed here. Similarly, the most favourable pathway with assistance of the *N*-$SO_3$ group has been carefully analysed in reference.[20] All the molecular geometries and energies of the TSs as calculated are listed in the Supporting Information (see footnote on the first page of this article).

### Reaction between the APA Model and Methylamine

In agreement with previous calculations on 3α-carboxypenam,[16] water-assisted methylaminolysis of **APA** through the **$TS_{APA}$1** structure is less efficient than the amine-assisted process through **$TS_{APA}$2** (see Scheme 6), the computed $\Delta G_{solution}$ barriers being 33.5 and 28.4 kcal·mol$^{-1}$, respec-

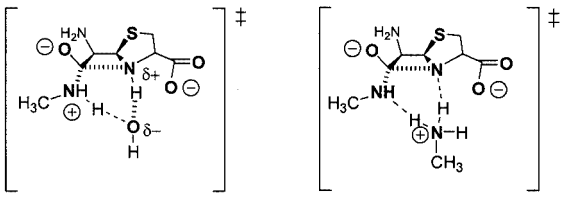


Scheme 6

Table 2. Relatives energies (kcal·mol$^{-1}$) with respect to reactants of the rate-determining transition structures considered in the aminolysis reactions studied theoretically

| β-Lactam | Nucleophile | Catalyst | | $\Delta E_{elec}$[a] | $\Delta G_{rot\text{-}vib}$[b] | $\Delta G_{cage}$[c] | $\Delta\Delta G_{solvation}$[d] | $\Delta G_{solution}$[e] |
|---|---|---|---|---|---|---|---|---|
| **APA** | $CH_3NH_2$ | **$H_2O$** | **$TS_{APA}$1** | 26.4 | 4.8 | 2.4 | −0.1 | 33.5 |
| **APA** | $CH_3NH_2$ | $CH_3$**$NH_2$** | **$TS_{APA}$2** | 19.5 | 8.9 | 4.8 | −4.8 | 28.4 |
| **APA** | $CH_2OHCH_2NH_2$ | (nucleophile)-**OH** | **$TS_{APA}$3** | 33.7 | 4.2 | 2.4 | −6.1 | 34.2 |
| **APA** | $CH_2OHCH_2NH_2$ | **$H_2O$** | **$TS_{APA}$4a** | 19.3 | 5.6 | 2.4 | 3.0 | 30.3 |
| **APA** | $CH_2OHCH_2NH_2$ | **$H_2O$** | **$TS_{APA}$4b** | 29.6 | 2.4 | 2.4 | −3.5 | 30.9 |
| **APA** | $CH_2OHCH_2NH_2$ | **$H_2O$** | **$TS_{APA}$4c** | 25.7 | 4.3 | 2.4 | 3.5 | 35.9 |
| **APA** | $CH_2OHCH_2NH_2$ | $CH_2OHCH_2$**$NH_2$** | **$TS_{APA}$5a** | 15.4 | 7.1 | 4.8 | 13.1 | 40.4 |
| **APA** | $CH_2OHCH_2NH_2$ | $CH_2OHCH_2$**$NH_2$** | **$TS_{APA}$5b** | 2.8 | 10.4 | 4.8 | 17.3 | 35.3 |
| **APA** | $CH_2OHCH_2NH_2$ | $CH_2OHCH_2$**$NH_2$** | **$TS_{APA}$5c** | 16.3 | 7.0 | 4.8 | 6.7 | 34.8 |
| **APA** | $CH_2OHCH_2NH_2$ | $CH_2OHCH_2$**$NH_2$** | **$TS_{APA}$5d** | 17.1 | 7.7 | 4.8 | 4.3 | 33.9 |
| **APA** | $CH_2OHCH_2NH_2$ | $CH_2OHCH_2$**$NH_2$** | **$TS_{APA}$5e** | 4.8 | 11.8 | 4.8 | 13.5 | 34.9 |
| **APA** | $CH_2OHCH_2NH_2$ | $CH_2OHCH_2$**$NH_2$** | **$TS_{APA}$5f** | 25.6 | 5.7 | 4.8 | −3.1 | 33.0 |
| **APA** | $CH_2OHCH_2NH_2$ | $CH_2$**OH**$CH_2NH_2$ | **$TS_{APA}$6** | 12.2 | 6.9 | 4.8 | 12.6 | 36.5 |
| **APA** | $CH_2OHCH_2NH_2$ | $CH_2$**OH**$CH_2NH_3^+$ | **$TS_{APA}$6-$H^+$** | *−48.4* | *6.9* | 4.8 | *69.5* | *32.8* |
| **MONO** | $CH_3NH_2$ | (β-lactam)-N**$SO_3^-$** | **$TS_{MONO}$1** | 23.9 | 4.6 | 2.4 | −0.8 | 30.1 |
| **MONO** | $CH_3NH_2$ | (β-lactam)-N**$SO_3^-$** | **$I_{MONO}$2** | 22.6 | 5.5 | 2.4 | −1.0 | 29.5 |
| **MONO** | $CH_3NH_2$ | (β-lactam)-N**$SO_3^-$** | **$TS_{MONO}$3** | 22.7 | 6.3 | 2.4 | 3.9 | 35.3 |
| **MONO** | $CH_3NH_2$ | **$H_2O$** | **$TS_{MONO}$4** | 22.0 | 6.3 | 2.4 | −0.6 | 30.1 |
| **MONO** | $CH_3NH_2$ | $CH_3$**$NH_2$** | **$TS_{MONO}$5** | 20.9 | 9.8 | 4.8 | −9.1 | 26.4 |
| **MONO** | $CH_3NH_2$ | $CH_3$**$NH_2$** & (β-lactam)-$NSO_3^-$ | **$TS_{MONO}$6** | 19.0 | 7.1 | 4.8 | −2.4 | 28.5 |
| **MONO** | $CH_3NH_2$ | $CH_3$**$NH_2$** & (β-lactam)-$NSO_3^-$ | **$I_{MONO}$7** | 15.7 | 7.4 | 4.8 | 7.5 | 35.4 |
| **MONO** | $CH_3NH_2$ | $CH_3$**$NH_2$** & (β-lactam)-$NSO_3^-$ | **$TS_{MONO}$8** | 16.3 | 7.3 | 4.8 | 10.4 | 38.8 |
| **MONO** | $CH_2OHCH_2NH_2$ | (nucleophile)-**OH** | **$TS_{MONO}$9** | 31.3 | 5.2 | 2.4 | −4.4 | 34.5 |
| **MONO** | $CH_2OHCH_2NH_2$ | **$H_2O$** | **$TS_{MONO}$10** | 20.4 | 5.7 | 2.4 | −3.4 | 25.1 |
| **MONO** | $CH_2OHCH_2NH_2$ | $CH_2OHCH_2$**$NH_2$** | **$TS_{MONO}$11** | 26.3 | 7.6 | 4.8 | −9.9 | 28.8 |
| **MONO** | $CH_2OHCH_2NH_2$ | $CH_2$**OH**$CH_2NH_2$ | **$TS_{MONO}$12** | 12.0 | 7.9 | 4.8 | 19.3 | 44.0 |
| **MONO** | $CH_2OHCH_2NH_2$ | $CH_2$**OH**$CH_2NH_3^+$ | **$TS_{MONO}$12-$H^+$** | *−48.9* | *7.9* | *4.8* | *71.7* | *35.5* |

[a] B3LYP/6-31+G* energies. [b] From B3LYP/6-31+G* frequencies. [c] Estimated as shown in ref.[29]. [d] Single-point HF/6-31+G* PCM SCRF on the gas phase B3LYP/6-31+G* geometries. [e] $\Delta G_{solution} = \Delta E_{elec} + \Delta G_{rot\text{-}vib} + \Delta G_{cage} + \Delta\Delta G_{solvation}$.

  

tively (see Table 2). The corresponding energy difference of 5.1 kcal·mol$^{-1}$ is the result of the placement of a positive charge on the catalytic amine, which in turn results in a more favourable electrostatic interaction with the β-lactam carboxylate and an important polarisation of the solvent continuum.

### Reaction between the APA Model and Ethanolamine Assisted by the Ethanolamine Hydroxy Group

The corresponding TS structure for this mechanism (**TS$_{APA}$3**, see Scheme 7) has an energy barrier of 34.2 kcal·mol. **TS$_{APA}$3** presents a relatively high $\Delta E_{elec}$ barrier (33.7 kcal·mol$^{-1}$), which reflects the unfavourable *syn* conformation adopted by the ethanolamine moiety in order to assist proton transfer from the attacking amino group to the β-lactam N atom.

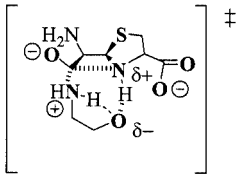

**TS$_{APA}$3**

Scheme 7

### Reaction between the APA Model and Ethanolamine Assisted by Water

Three different conformers of the water-assisted TS were located (**TS$_{APA}$4a**, **TS$_{APA}$4b**, and **TS$_{APA}$4c**), with $\Delta G_{solution}$ energy barriers of 30.3, 30.9, and 35.9 kcal·mol$^{-1}$, respectively. These TS structures, which correspond to concerted processes on the B3LYP/6-31+G* PES, basically differ in the conformation of the hydroxy group of the nucleophile (see Scheme 8). The lowest energy barrier corresponds to **TS$_{APA}$4a**, in which the ethanolamine hydroxy group interacts with the catalytic water molecule through a short hydrogen bond (O−H···O = 1.662 Å).

### Reaction between the APA Model and Ethanolamine Assisted by a Second Amine Molecule

For the reaction between **APA** and ethanolamine catalysed by the amine group of a second ethanolamine molecule, six concerted TS structures with different conformations, both of the nucleophilic and of the ancillary ethanolamine molecules, were located (see Scheme 9). In this case, the lowest $\Delta E_{elec}$ barrier (only 2.8 kcal·mol$^{-1}$) corresponds to **TS$_{APA}$5b**, in which the carboxylate β-lactam group establishes a short hydrogen bond (O···O = 2.63 Å) with the hydroxy group of the catalytic moiety. However, this arrangement of the polar groups is strongly disfavoured by solvent effects according to the PCM calculations ($\Delta\Delta G_{solvation}$ = +17.3 kcal·mol$^{-1}$), the overall energy barrier being 35.3 kcal·mol$^{-1}$. Reciprocally, if the hydroxy groups

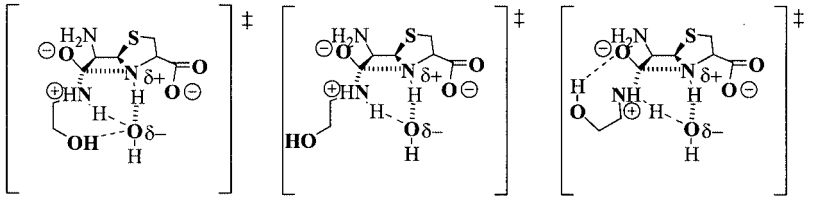

**TS$_{APA}$4a** **TS$_{APA}$4b** **TS$_{APA}$4c**

Scheme 8

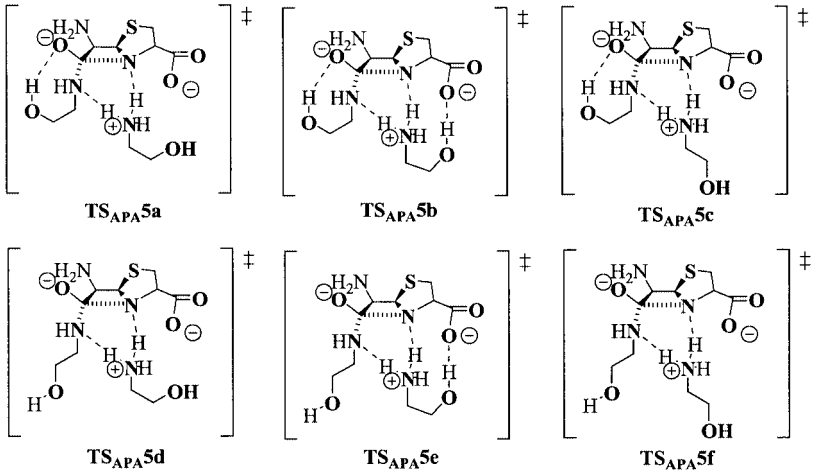

**TS$_{APA}$5a** **TS$_{APA}$5b** **TS$_{APA}$5c**

**TS$_{APA}$5d** **TS$_{APA}$5e** **TS$_{APA}$5f**

Scheme 9

  

of both the nucleophilic and catalytic amines are simultaneously oriented towards the solvent continuum at **$TS_{APA}$5f**, the intrinsic energy barrier is much larger ($\Delta E_{elec}$ = 25.6 kcal·mol$^{-1}$) and there is no desolvation penalty ($\Delta\Delta G_{solvation}$ = −3.1 kcal·mol$^{-1}$). Overall, the latter conformer, **$TS_{APA}$5f**, is predicted to be the most stable TS, with a global $\Delta G_{solution}$ barrier of 33.0 kcal·mol$^{-1}$, although this is only 1.3 and 2.3 kcal·mol$^{-1}$ below **$TS_{APA}$5b** and **$TS_{APA}$5e**, respectively.

### Reaction between the MONO Model and Methylamine Assisted by the β-Lactam N-$SO_3^-$ Group

The *N*-$SO_3^-$-assisted mechanism proceeds in a stepwise manner, passing through an open-chain intermediate (see Scheme 3).[20] The rate-determining event through which the β-lactam ring is cleaved, thus forming the open-chain intermediate, has been characterized.[20] In order for this process to occur, *two* transition states (**$TS_{MONO}$1** and **$TS_{MONO}$3**) and a tetrahedral intermediate (**$I_{MONO}$2**) were located; these are very similar geometrically and energetically in the gas phase. If solvent effects are taken into account, **$TS_{MONO}$3** becomes the highest critical structure along the $\Delta G_{solution}$ profile, given that it has a much less ionic character than those exhibited by **$TS_{MONO}$1** and the tetrahedral intermediate. The global $\Delta G_{solution}$ for the *N*-$SO_3^-$-assisted mechanism amounts to 35.3 kcal·mol$^{-1}$.

To discover whether a second amine molecule and the *N*-$SO_3^-$ group could catalyse the cleavage of the monobactam ring more efficiently together, a nucleophilic attack of one amine molecule concomitant with proton transfer from the nucleophilic amine to the *N*-sulfonate group assisted by the second amine molecule was simulated. Three critical structures were located: two TSs and a closed-ring tetrahedral intermediate (i.e., **$TS_{MONO}$6** → **$I_{MONO}$7** → **$TS_{MONO}$8**). These are very close both in energy and structure [see Table 2 and the Supporting Information (see footnote on the first page of this article)]. We found that the presence of the ancillary amine molecule increases the desolvation penalty both of the tetrahedral intermediate **$I_{MONO}$7** and of **$TS_{MONO}$8**, which are less stable in solution than **$TS_{MONO}$6** by 6.9 and 10.3 kcal·mol$^{-1}$, respectively. Overall, this mechanism is not competitive with the *N*-$SO_3^-$-assisted mechanism passing through **$TS_{MONO}$3**.

### Reaction between the MONO Model and Methylamine Assisted by Water or by a Second Amine Molecule

With regard to water-assisted (**$TS_{MONO}$4**) and amine-assisted (**$TS_{MONO}$5**) aminolysis of the **MONO** model, the corresponding TSs at the B3LYP/6-31+G* level are analogous to those obtained for the **APA** model (**$TS_{APA}$1** and **$TS_{APA}$2**). The calculations performed predict that the methylamine-assisted process passing through **$TS_{MONO}$5** ($\Delta G_{solution}$ = 26.4 kcal·mol$^{-1}$) is 3.7 kcal·mol$^{-1}$ more favourable than the water-assisted processes ($\Delta G_{solution}$ = 30.1 kcal·mol$^{-1}$). Both **$TS_{MONO}$4** and **$TS_{MONO}$5** are more stable in aqueous solution than **$TS_{MONO}$3**, by 5.2 and 8.9 kcal·mol$^{-1}$, so the *N*-$SO_3^-$ assisted process would not be competitive.

### Reaction between the MONO Model and Ethanolamine

Three one-step mechanisms were considered for the reaction between **MONO** and ethanolamine, with catalysis involving: (a) the ethanolamine hydroxy group, (b) a water molecule, and (c) a second ethanolamine (i.e., the *N*-$SO_3$-assisted pathway was not considered). The first mechanism with intramolecular catalysis has an estimated barrier of 34.5 kcal·mol$^{-1}$ in solution. For the water- and amine-assisted processes, the conformations of the ethanolamine molecules in the corresponding TSs are similar to those shown by the most stable TS conformers located for the **APA**-ethanolamine system. The computed $\Delta G_{solvation}$ barriers are only 25.1 kcal·mol$^{-1}$ (water-assisted) and 28.8 kcal·mol$^{-1}$ (amine-assisted).

### Comparison between Theoretical and Experimentally Measured Results

To find out whether the theoretical description of aminolysis of β-lactams achieved is consistent with the basic kinetic trends revealed by experimentally obtained kinetic results, the computed differences in the $\Delta G_{solution}$ barriers for the different model systems and reaction mechanisms were compared with experimentally ascertained differences in activation energies ($\Delta\Delta E_a^{exp}$). The $\Delta\Delta E_a^{exp}$ values were derived from Arrhenius's equation, with a common pre-exponential factor being assumed for all aminolysis processes. The $\Delta\Delta G_{solution}$ and $\Delta\Delta E_a^{exp}$ terms, which characterise the kinetic preference for the $k_1$ over the $k_2$ route as well as the kinetic impact of the β-lactam (penicillin vs. monobactam) and the nucleophile (methylamine versus ethanolamine), are laid out in Tables 3−5.

### Kinetic Preference for the Water-Assisted Route over the Amine-Assisted Route

In previous work[15] it was proposed that the water-assisted mechanism is the most important contribution to the $k_1$ term for the aminolysis of β-lactams. This proposal is further supported by these calculations on the **APA** and **MONO** model systems. For the aminolysis of monobactams, for example, the water-assisted route turns out to be 5.2 kcal·mol$^{-1}$ more favourable than the *N*-$SO_3^-$ assisted process. Similarly, the intramolecularly catalysed pathway for reactions between β-lactams and ethanolamine would not be competitive. Therefore, if the experimentally determined kinetic term proportional to [amine] ($k_1$) is interpreted as being in fact catalysed by water, in consonance with the theoretical results, the observed rate constant $k_1$ should be divided by 55 M (i.e., the concentration of pure water) before comparison with the other kinetic constant $k_2$.[22] This has been done in order to derive the experimental $\Delta\Delta E_a^{exp}$ values reported in Table 3.

  

Table 3. Kinetic preference of the water-assisted route ($k_1$) relative to the mechanism assisted by a second amine molecule ($k_2$) as estimated from experimental rate constants and quantum chemical calculations. $\Delta\Delta E_a$ and $\Delta\Delta G$ values in kcal·mol$^{-1}$

| β-Lactam | Nucleophile | $\Delta E(k_1) - \Delta E(k_2)$ $\Delta\Delta E_a^{exp} \approx -RT\ln[(k_1/55M)/k_2]$ | $\Delta\Delta G_{solution}$ |
|---|---|---|---|
| **APA** | $RNH_2$[a] | 5.6 | 5.1 |
| **APA** | $CH_2OHCH_2NH_2$ | 3.3 | *−2.7* |
| **MONO** | $RNH_2$[a] | 4.1 | 3.7 |
| **MONO** | $CH_2OHCH_2NH_2$ | 4.5 | *−3.8* |

[a] R = $CH_3CH_2CH_2$- (exp.)/$CH_3$- (theor.).

Experimentally, all the kinetic data indicate that the amine-assisted route ($k_2$) is clearly more favourable than the water-assisted mechanism ($k_1$), by ca. 3−6 kcal·mol$^{-1}$. This kinetic preference is very well reproduced by the calculations for the reactions between methylamine and either **APA** or **MONO** (see Table 3). Moreover, analyses of the different energy components contributing to $\Delta G_{solution}$ allow this kinetic preference to be unequivocally interpreted in terms of solvent effects stabilizing the catalytic methylammonium moiety at the corresponding amine-assisted TSs (for example, $\mathbf{TS_{APA}2}$ is significantly stabilized by solvent, having a $\Delta\Delta G_{solvation}$ value of −4.8 kcal·mol$^{-1}$; see Table 2). In contrast, the calculated $\Delta\Delta G_{solution}$ values corresponding to the reactions between **APA/MONO** and ethanolamine are qualitatively incorrect (−2.7/−3.8 kcal·mol$^{-1}$) when compared with the $\Delta\Delta E_a^{exp}$ values for 6-APA and aztreonam (3.3 and 4.5 kcal·mol$^{-1}$, respectively). This discrepancy can be traced to an overestimation of the desolvation penalty by the HF/6-31+G* SCRF PCM calculations when *two* molecules of ethanolamine are present in the same solvent cage. Moreover the B3LYP/6-31+G* level may well overestimate the short hydrogen bond interaction between the nucleophilic ethanolamine and the catalytic water molecule at $\mathbf{TS_{APA}4a}$ and $\mathbf{TS_{MONO}10}$.

### Influence of the β-Lactam Structure

From the experimentally derived results summarized in Table 1, it seems that, in the cases studied here, the β-lactam structure has a moderate influence over the kinetic constants $k_1$ and $k_2$, but in a different manner. For the water-assisted processes ($k_1$), this effect also depends on the nature of the nucleophile: aztreonam reacts more rapidly than 6-APA with propylamine ($\Delta\Delta E_a^{exp}$ = 2.1 kcal·mol$^{-1}$), but it is slightly slower in reacting with ethanolamine ($\Delta\Delta E_a^{exp}$ = −0.3 kcal·mol$^{-1}$). On the other hand, aztreonam is consistently slightly more reactive by the amine-assisted pathway, by 0.5 and 0.7 kcal·mol$^{-1}$.

The computed $\Delta\Delta G_{solution}$ values for the **APA** and **MONO** systems predict that the monobactam structure should be more reactive than the penicillin model by ca. 2−5 kcal·mol$^{-1}$ in all reactions considered. This theoretical prediction *qualitatively* reproduces the experimentally observed kinetic trend shown by the $\Delta\Delta E_a^{exp}$ terms for propylamine. In contrast, the calculations performed here do not account for the small experimentally observed kinetic effects of the β-lactam structure for the reaction processes with ethanolamine, particularly in the case of the water-assisted pathway ($k_1$ route, see Table 4). This was not entirely unexpected, given that the relative stability of the $\mathbf{TS_{MONO}10}$ structure seems most probably to be overestimated by our theoretical calculations (see above). Nevertheless, it does appear that the calculations can help understanding of the kinetic effects of the β-lactam structure. Thus, the relative positions of the carboxylate/*N*-sulfonate groups with respect to the reactive amide bond and the $OH^-/RNH_3^+$-*like* catalytic moieties could affect both the intrinsic stability of the TSs and their interaction with the solvent continuum. For example, inspection of the $\Delta E_{elec}$ and $\Delta\Delta G_{solvation}$ energy components in Table 2 for the amine-assisted processes shows that the *N*-$SO_3^-$ group of **MONO** increases the $\Delta E_{elec}$ energy barrier and simultaneously reinforces solvent stabilization with respect to the **APA** system. The latter effect dominates, thus explaining the higher reactivity of **MONO** through the $k_2$ route. On the other hand, most of the monobactam rate enhancement in the water-assisted reaction with propylamine could be due to weaker repulsion between the hydroxide-like moiety and the *N*-$SO_3$ group than between the hydroxide−like moiety and the carboxylate group of 6-APA.

Table 4. Kinetic influence of the β-lactam structure on the aminolysis mechanisms ($k_1$ and $k_2$) as estimated from experimental rate constants and quantum chemical calculations. $\Delta\Delta E_a$ and $\Delta\Delta G$ values in kcal·mol$^{-1}$

| Mechanism | Nucleophile | $\Delta E$ (**APA**) − $\Delta E$ (**MONO**) $\Delta\Delta E_a^{exp} \approx -RT\ln(k^{APA}/k^{MONO})$ | $\Delta\Delta G_{solution}$ |
|---|---|---|---|
| $k_1$ | $RNH_2$[a] | 2.1 | 3.4 |
| $k_1$ | $CH_2OHCH_2NH_2$ | −0.3 | *5.2* |
| $k_2$ | $RNH_2$[a] | 0.5 | 2.0 |
| $k_2$ | $CH_2OHCH_2NH_2$ | 0.7 | 4.2 |

[a] R = $CH_3CH_2CH_2$- (exp.)/$CH_3$-(theor.).

### Influence of the Nucleophile

The experimentally obtained data in Tables 1 and 5 reveal that ethanolamine is, in general, less reactive than propylamine during the aminolysis of both 6-APA and aztreonam, with $\Delta\Delta E_a^{exp} = \approx -1, -2$ kcal·mol$^{-1}$. There is, however, one exception, corresponding to the water-assisted ($k_1$) aminolysis of 6-APA, in which ethanolamine turns out to be a better nucleophile ($\Delta\Delta E_a^{exp} = +0.8$). Theoretical calculations on the **APA** and **MONO** model systems predict the same kinetic trends, except for the $k_1$ route in the monobactam model.

Common interpretations assume that the nucleophilic strengths of the monoamines are correlated with their p$K_a$ values, hence explaining the lower reactivity of ethanol-

  

Table 5. Kinetic influence of the nucleophile on the aminolysis mechanisms ($k_1$ and $k_2$) as estimated from experimental rate constants and quantum chemical calculations; $\Delta\Delta E_a$ and $\Delta\Delta G$ values in kcal·mol$^{-1}$

| Mechanism | β-Lactam | $\Delta E(RNH_2^{[a]}) - \Delta E(CH_2OHCH_2NH_2)$ $\Delta\Delta E_a^{exp} \approx -RT\ln(k^{RNH2}/k^{CH2OHCH2NH2})$ | $\Delta\Delta G_{solution}$ |
|---|---|---|---|
| $k_1$ | **APA** | 0.8 | 3.2 |
| $k_1$ | **MONO** | −1.7 | *5.0* |
| $k_2$ | **APA** | −1.6 | −4.6 |
| $k_2$ | **MONO** | −1.4 | −2.4 |

[a] R = $CH_3CH_2CH_2-$ (exp.)/$CH_3-$ (theor.).

amine (p$K_a$ = 9.7) in relation to propylamine/methylamine (p$K_a$ = 10.6−10.7). Calculations for the amine-assisted processes performed in this work support this interpretation, given that the most stable TSs with ethanolamine have intrinsic energy barriers ($\Delta E_{elec}$) of ca. 4−5 kcal·mol$^{-1}$ higher than those of the equivalent TSs involving methylamine (see for example the **TS$_{APA}$2** and **TS$_{APA}$5f** energy components in Table 2). In these TSs the hydroxy groups of the ethanolamine molecules point toward the solvent bulk; that is, they do not interact with the reactive atoms. However, another TS conformer, in which the nucleophilic ethanolamine is hydrogen-bonded to the β-lactam carbonyl O atom, is only 1.9 less stable (**TS$_{APA}$5c**). The presence of this intramolecular hydrogen bond significantly reduces the $\Delta E_{elec}$ barrier, but impairs electrostatic solute-solvent interactions at the TS, increasing the $\Delta\Delta G_{solvation}$ term. Moreover, the most stable TS for the reaction between APA and one ethanolamine molecule (**TS$_{APA}$4a**) turns out to be largely stabilized by intramolecular OH···O contact between the ethanolamine moiety and the catalytic water, resulting in a low $\Delta E_{elec}$ barrier of 19.3 kcal·mol$^{-1}$. It therefore seems that the reactivity of ethanolamine is modulated by three factors: the intrinsic nucleophilicity of the attacking amino group, the ability of ethanolamine to provide intramolecular hydrogen-bonds, and also solvent effects. This combination of kinetic factors causes theoretical prediction of relative $\Delta G_{solution}$ values to be less trustworthy for ethanolamine than for methylamine reaction systems, owing to lesser "cancellation of errors".

### Bifunctional Catalysis Exerted by Ethanolammonium Molecules

In principle, the experimentally detected kinetic term in the rate law proportional to [$CH_2OHCH_2NH_2$]-[$CH_2OHCH_2NH_3^+$] can be interpreted in terms of a mechanism in which the nucleophilic attack by the neutral amine molecule would be assisted by the hydroxy group of the protonated amine molecule through bifunctional catalysis. The question naturally arose of whether theoretical calculations could support this hypothesis.

Unfortunately, the presence of the charged ammonium group in $CH_2OHCH_2NH_3^+$ makes B3LYP/6-31+G* geometry optimisations in the gas phase unrealistic for simulation of the actual reaction in solution, owing to charge neutralisation between the β-lactam carboxylate and the positively charged amine molecule. To circumvent this difficulty, it was decided first to investigate the reactions between the **APA/MONO** models and ethanolamine catalysed by the hydroxy group of a second ethanolamine molecule in its basic (uncharged) form. The corresponding TS structures, fully optimized on the B3LYP/6-31+G* PES, were then neutralised by attachment of a proton to the free amino end of the catalytic fragment while the geometry of the rest of the system was kept frozen (see Scheme 10). Subsequently, single-point B3LYP/6-31+G* and HF/6-31+G*-SCRF PCM calculations were performed on the neutralised structures. In this way, it proved possible to estimate the $\Delta G_{solution}$ barriers corresponding to aminolysis of **APA/MONO** assisted by the positively charged $CH_2OHCH_2NH_3^+$ molecule. The energetic results are collected in Table 2, while views of the optimized structures used in these calculations are included in the Supporting Information.

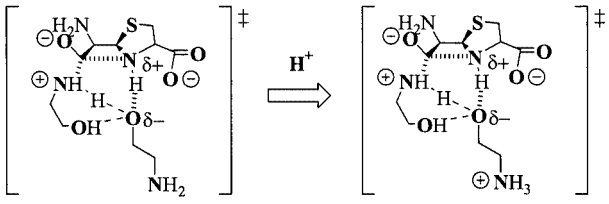


Scheme 10

In the neutral and fully-optimized TSs with catalysis by the hydroxy group of the second ethanolamine molecule (**TS$_{APA}$6** and **TS$_{MONO}$12**), the nucleophilic ethanolamine is hydrogen-bonded to the catalytic hydroxy moiety of the second ethanolamine molecule (as in the comparable water-assisted TSs) while the free amino group of the catalytic ethanolamine points towards the solvent continuum. The $\Delta G_{solution}$ barriers computed for **TS$_{APA}$6** and **TS$_{MONO}$12** are quite high: 36.5 and 44.0 kcal·mol$^{-1}$, respectively. The magnitude of these values confirms that the ethanolamine hydroxy group is a worse catalyst than the amino group, in all probability because of worse solvent stabilization of the $NH_2CH_2CH_2O^-$ catalytic moiety than of the ammonium-*like* $NH_3^+CH_2CH_2OH$ (see the $\Delta\Delta G_{solvation}$ values in Table 2). Both **TS$_{APA}$6** and **TS$_{MONO}$12** were converted into their protonated counterparts (**TS$_{APA}$6-H$^+$** and **TS$_{MONO}$12-H$^+$**) by attachment of a proton to the amino of the catalytic moiety. Although relaxation effects upon the protonation process were neglected, the estimated $\Delta G_{solution}$ barriers were quite moderate: 32.8 and 35.5 kcal·mol$^{-1}$ for the **APA** and **MONO** model compounds. Quite remarkably, these figures are very close to $\Delta G_{solution}$ barriers corresponding to the ethanolamine-assisted processes (**TS$_{APA}$5** and **TS$_{MONO}$11**), thus suggesting that the protonated $CH_2OHCH_2NH_3^+$ molecules may have an active kinetic role as bifunctional catalysts during the aminolysis of β-lactam antibiotics.

  

### Summary and Conclusions

Kinetic experiments have been performed in order to characterise the reactivity of monobactam antibiotics (aztreonam) against amine nucleophiles relative to that of penicillin compounds (6-APA). The magnitude of the experimentally determined kinetic constants [$k_1$, $k_2$, and $k_3$ appearing in the rate law in Equation (1)] shows that aztreonam is slightly more reactive than 6-APA, despite common assumptions that the amide bond should be less activated in monobactams. It may be interesting to note that these kinetic results are consistent with the experimentally determined rate for aztreonam covalent linkage to the ε-amino groups of lysine residues in HSA plasma proteins (70% of the initial aztreonam fixed to HSA after 24 hours of reaction[23]), which is higher than that reported for benzylpenicillins (3% after 48 hours[24]). Furthermore, the kinetic influence of substitution on the attacking nucleophile was also investigated. Most remarkably, for ethanolamine in reaction with either aztreonam or 6-APA, the corresponding rate law has a kinetic term proportional to $[RNH_2][RNH_3^+]$, in contrast with previous reports on the reaction between benzylpenicillin and ethanolamine.[9]

To gain a better understanding of the various effects controlling the rates of the reactions between β-lactams and amines, the molecular details of the reactive processes were investigated by quantum chemical calculations. The **APA** and **MONO** model systems shown in Scheme 5 were considered in order to compute the rate-determining $\Delta G_{solution}$ barriers corresponding to various reaction mechanisms, all involving bifunctional catalysis by water, a second amine molecule or the *N*-sulfonate groups of monobactams (the electronic and geometrical features of these mechanisms have been discussed in previous theoretical work[15,20]).

The theoretical results confirm the ability of the water-assisted ($k_1$) and amine-assisted ($k_2$) mechanisms to explain experimental data on the aminolysis of β-lactams. Thus, the computed $\Delta G_{solution}$ barriers have moderate values ranging from ca. 26 to ca. 34 kcal·mol$^{-1}$. For the aminolysis of monobactams, the previously proposed *N*-$SO_3^-$-assisted mechanism[20] turns out to be 5.2 kcal·mol$^{-1}$ less stable than the water-assisted route. Moreover, the theoretical calculations undertaken here satisfactorily reproduce several experimentally observed kinetic trends: the prevalence of the amine-assisted mechanism ($k_2$ term in the rate law) over the water-assisted route ($k_1$) and the higher reactivity exhibited by the monobactam. Nevertheless, the most interesting prediction made by these calculations is that the kinetic term in the experimental rate law proportional to $[CH_2OHCH_2NH_2]\cdot[CH_2OHCH_2NH_3^+]$ can be interpreted in terms of the bifunctional catalysis performed by the hydroxy group of the protonated amine molecule. Finally, from comparison between experimental and theoretical data, it was concluded that combination of standard DFT gas-phase calculations with SCRF solvation methodologies can yield relative $\Delta G_{solution}$ barriers with semiquantitative accuracy and give valuable insights into the various factors controlling the rate of chemical processes in the condensed phase.

## Experimental Section

**Materials:** Aztreonam was supplied by Squibb & Sons, Inc. (New Jersey, U.S.A.). 6-Aminopenicillanic acid (6-APA), propylamine and ethanolamine were obtained from SIGMA-ALDRICH CHEMIE GmbH (Germany). The amines were purified by distillation prior to use. Other chemicals were commercial products of analytical grade. All the water used was purified by a Milli-Q-Reagent Water System (Millipore Bedford, MA, U.S.A.).

**Analytical Procedure:** The residual antibiotic concentration was determined by a reversed-phase high-performance liquid chromatography (RP-HPLC) method. An Alliance® HPLC System liquid chromatograph (Waters, Mildford, MA, U.S.A.) equipped with a 2695 Separations Module and a 996 Photodiode Array Detector were used. The separation was carried out with a Phenomenex C18 (2) Luna Column (5μm; 150 × 4.60 mm). The mobile phase used was as follows: 0.05 M, pH 6.50, sodium phosphate/methanol solution (84:16, v/v). The flow rate was maintained at 1 mL·min$^{-1}$. All separations were carried out at ambient temperature and detection of antibiotics was performed at 237 nm. The mobile phases were prepared fresh on the day of analysis and were filtered through a Millipore filter (0.45-μm. pore size). The β-lactam compounds were determined by comparison of the peak areas with those of similarly chromatographed standards. Calibration curves for the β-lactam compounds were prepared daily.

**Kinetic Procedure:** The amines were used both as buffers and as nucleophiles. The solutions were freshly prepared and the pH values were measured at 30 °C by use of a WTW pH-meter (pH, 526) equipped with a combined electrode with integrated temperature sensor (Sentix 97T). All reactions were conducted at 30.0±0.1 °C, and the ionic strength was adjusted to 0.25 M with potassium chloride. In some cases in which buffer capacity was too low, the pH of the kinetic solution during the reaction was maintained with a pH-stat (Titrimeter assembly consisting of a E-614 Impulsomat, a E-655 Dosimat and a E-632 pH-meter from Metrohm, Herisau, Switzerland).

The initial β-lactam compound concentration was $1-2\times10^{-4}$ mol·L$^{-1}$. Samples of reaction solutions were withdrawn at appropriate time intervals and the β-lactam compound remaining was analysed by HPLC. The observed pseudo-first order rate constants, $k_{obs}$, were calculated by a generalised least-squares method and the values of other rate constants were derived by a linear least-squares method.

**Ionization Constants:** The p$K_a$ values used for the calculation were reported values.[9] The p$K_a$ of propylamine was 10.79 and that of ethanolamine was 9.73. Hydroxide ion concentration was taken as antilog (pH − p$K_w$) with p$K_w$= 13.83.[9]

**Computation:** Molecular geometry optimisations followed by analytical frequency calculations were performed at the B3LYP/6-31+G* level of theory[25,26] by use of the Gaussian 98 suite of programs.[27] In previous work on the aminolysis of 2-azetidinone,[15,17] it had been discovered that the B3LYP density function combined with double-ζ basis sets provides relative electronic energies ($\Delta E_{elec}$) quite close (±1, 2 kcal·mol$^{-1}$) to those predicted by the G2(MP2,SVP) composite approach,[28] which takes account of the effect of larger basis sets and more refined *N*-electron treatments.

  

To take account of condensed-phase effects on the kinetics of the reaction, we used the UAHF (united atom Hartree−Fock) parameterisation[29] of the polarizable continuum model[30] (PCM) including both electrostatic and non-electrostatic solute-solvent interactions and simulating water as solvent. The HF method combined with a double-ζ basis set and the UAHF PCM model reproduces the experimental solvation energies of 43 neutral molecules and 27 ions well, with mean errors of 0.2 and 1 kcal·mol$^{-1}$ for neutral solutes and ions, respectively.[29] For example, the HF/6-31+G** solvation energies (with the gas-phase B3LYP/6-31+G** geometries) for $OH^-$, $CH_3O^-$, $CH_3COO^-$, $CH_3NH_3^+$ are −108, −93, −79, and −70 kcal/mol, respectively, which compare quite well with the corresponding experimentally determined values of −106, −95, −77, and −70 kcal·mol$^{-1}$. The corresponding B3LYP/6-31+G* UAHF PCM values are −104, −88, −75 and −71 kcal·mol$^{-1}$, so B3LYP tends to underestimate the solvation energies of anions, particularly that of the alkoxide $CH_3O^-$. The Gibbs energies of solvation ($\Delta G_{solvation}$) of all the critical structures reported in this work were therefore then computed from single-point HF/6-31+G* PCM-UAHF calculations on the B3LYP/6-31+G* gas-phase geometries. It should also be noted that the topologies of the systems were controlled so that the UAHF radii of all the atoms was the same in analogous structures. The SCRF calculations were carried out with the gas-phase geometries, since similar optimized geometries had been found both in the gas phase and in solution in previous work on the aminolysis of 2-azetidinone.[31] Furthermore, in the same work,[31] the relative $\Delta G_{solvation}$ values for the structures along the reaction energy profile were practically identical, regardless of the geometries used (i.e., whether gas-phase or solvated geometries). Similar observations have been reported for the ammonolysis of formic acid.[19]

In order to estimate the free energy barrier in aqueous solution ($\Delta G_{solution}$) for the aminolysis processes, various energy terms were combined in accordance with the following Equation (3).

$$\Delta G_{solution} = \Delta E_{elec} + \Delta G_{rot,vib}^{gas-phase} + \Delta\Delta G_{solvation} + \Delta G_{cage} \quad (3)$$

$\Delta E_{elec}$ is the energy difference at 0 K at the B3LYP/6-31+G* level, $\Delta G_{rot,vib}^{gas-phase}$ are the vibrational and rotational contributions evaluated within an ideal gas, rigid rotor, and harmonic oscillator approximations[32] and with the use of the B3LYP/6-31+G* analytical frequencies (the change in $\Delta G_{rot,vib}$ on going from the gas phase to solution is neglected), $\Delta\Delta G_{solvation}$ is the difference in the HF/6-31+G* SCRF PCM solvation energies between the TS structure and reactants, and $\Delta G_{cage}$ is a translational free energy contribution associated with the bringing of the reacting fragments into the same solvent cage. From the reference[33] it was assumed that $\Delta G_{cage}$ is determined solely by concentration factors: for standard conditions (1 M), $\Delta G_{cage}$ has a value of 2.4 kcal·mol$^{-1}$ for bringing two specific molecules next to each other if identical molar volumes are assumed (see reference[33] for full details). It is to be noted that this $\Delta G_{cage}$ term can be seen as an alternative to the inclusion of a free energy term evaluated in the gas phase (i.e., $\Delta G_{translational}^{gas-phase}$), which would strongly overestimate the entropic penalty of confining the reactants together in the condensed phase. Other definitions of $\Delta G_{cage}$ energy involving both vibrational and rotational degrees of freedom as well as the desolvation penalty have been proposed in the literature,[34] although theoretical computations are quite expensive, given that molecular dynamics simulations and potential of mean force calculations with appropriately selected restraints are required for each particular system.[35]

Unfortunately, agreement between ab initio absolute $\Delta G_{solution}$ barriers and experimentally measured values is notoriously difficult to achieve, mainly because very high levels of theory are required for accurate prediction of the $\Delta E_{elec}$ energies, but also in view of the uncertainties in the SCRF methodology, the approximate estimation of the $\Delta G_{cage}$ energy, and so forth. Thus, even small relative errors in the calculations can have very large effects on absolute rates. In practice, the estimation of relative $\Delta G_{solution}$ values of related systems can be carried out with much more confidence by use of quantum mechanical methods coupled with continuum models thanks to partial mutual cancelling out of errors.

**Supporting Information**

Figures showing the optimized geometries and energies of all the structures considered in this work (9 pages, see footnote on the first page of this article).

## Acknowledgments

We thank the MCyT for financial support (SAF2001−3526). We are also grateful to the MCyT for a generous allocation of computer time at the CESCA and the CIEMAT. The experimental work was carried out with the equipment in the Instrumental Techniques Laboratory of the University of León.

[1] B. B. Levine, Z. Ovary, *J. Exp. Med.* **1961**, *114*, 875−904.
[2] F. Moreno, M. Blanca, C. Mayorga, S. Terrados, M. Moya, E. Pérez, R. Suau, J. M. Vega, J. García, A. Miranda, M. J. Carmona, *Int. Arch. Allergy Immunol.* **1995**, *108*, 74−81.
[3] A. Saxon, E. A. Swabb, N. F. J. Adkinson, *Am. J. Med* **1985**, *78 (Suppl 2A)*, 19−26.
[4] M. A. Schwartz, G. M. Wu, *J. Pharm. Sci.* **1966**, *55*, 550−555.
[5] H. Bundgaard, *Arch. Pharm. Chem. Sci. Ed.* **1975**, *3*, 94−97.
[6] A. Tsuji, T. Yamana, F. Miyamoto, E. Kiya, *J. Pharm. Pharmacol.* **1975**, *27*, 580−587.
[7] T. Yamana, A. Tsuji, E. Miyamoto, E. Kiya, *J. Pharm. Pharmacol.* **1975**, *27*, 56−57.
[8] G. M. Blackburn, J. D. Plackett, *J. Chem. Soc., Perkin Trans. 2* **1973**, 981−985.
[9] J. J. Morris, M. I. Page, *J. Chem. Soc., Perkin Trans. 2* **1980**, 212−219.
[10] J. J. Morris, M. I. Page, *J. Chem. Soc., Perkin Trans. 2* **1980**, 220−224.
[11] M. I. Page, *Acc. Chem. Res.* **1984**, *17*, 144−151.
[12] J. Martín, R. Méndez, T. Alemany, *J. Chem. Soc., Perkin Trans. 2* **1989**, 223−227.
[13] M. I. Page, in: *The Chemistry of β-lactams.* (Ed.: M. I. Page), Blackie Academic & Professional, London, **1992**, pp. 129−147; and references cited therein.
[14] C. D. Richtie, *Physical Organic Chemistry*, Marcel Dekker Inc., New York, **1990**.
[15] N. Díaz, D. Suárez, T. L. Sordo, *J. Am. Chem. Soc.* **2000**, *122*, 6710−6719.
[16] N. Díaz, D. Suárez, T. L. Sordo, *Eur. J. Org. Chem.* **2001**, 793−801.
[17] N. Díaz, D. Suárez, T. L. Sordo, *J. Org. Chem.* **1999**, *64*, 9144−9152.
[18] N. Díaz, PhD thesis, Universidad de Oviedo (Oviedo), **2001**.
[19] S. Chalmet, W. Harb, M. F. Ruiz-López, *J. Phys. Chem. A* **2001**, *105*, 11574−11581.
[20] N. Díaz, D. Suárez, T. L. Sordo, *Helvetica Chimica Acta* **2002**, *85*, 206−223.
[21] M. B. Diender, A. J. J. Straathof, L. A. M. van der Wielen, C. Ras, J. J. Heijnen, *J. Mol. Catalysis B: Enzymatic* **1998**, *5*, 249−253.
[22] W. P. Jencks, *Catalysis in Chemistry and Enzymology*, Dover Publications, Inc., New York, **1987**.

  

[23] N. F. Adkinson, E. Swaab, A. A. Sugerman, *Antimicrob. Agents. Chemother* **1984**, *23*, 93−97.
[24] F. R. Batchelor, J. M. Dewdney, D. Gazzard, *Nature* **1965**, *206*, 362−364.
[25] A. D. Becke, in: *Modern Electronic Structure Theory Part II* (Ed.: D. R. Yarkony), World Scientific, Singapore, **1995**.
[26] W. J. Hehre, L. Radom, P. v. R. Schleyer, J. A. Pople, *Ab Initio Molecular Orbital Theory*, John Wiley & Sons, New York, **1986**.
[27] M. J. Frisch, G. W. Trucks, H. B. Schlegel, G. E. Scuseria, M. A. Robb, J. R. Cheeseman, V. G. Zakrzewski, J. A. Montgomery, J. Stratmann, R. E., J. C. Burant, S. Dapprich, J. M. Millam, A. D. Daniels, K. N. Kudin, M. C. Strain, O. Farkas, J. Tomasi, V. Barone, M. Cossi, R. Cammi, B. Mennucci, C. Pomelli, C. Adamo, S. Clifford, J. Ochterski, G. A. Petersson, P. Y. Ayala, Q. Cui, K. Morokuma, D. K. Malick, A. D. Rabuck, K. Raghavachari, J. B. Foresman, J. Cioslowski, J. V. Ortiz, B. B. Stefanov, G. Liu, A. Liashenko, P. Piskorz, I. Komaromi, R. Gomperts, R. L. Martin, D. J. Fox, T. Keith, M. A. Al-Laham, C. Y. Peng, A. Nanayakkara, C. Gonzalez, M. Challacombe, P. M. W. Gill, B. Johnson, W. Chen, M. W. Wong, J. L. Andres, C. Gonzalez, M. Head-Gordon, E. S. Replogle, J. A. Pople, *Gaussian 98, A.6 ed.,* Pittsburgh PA, **1998**.
[28] L. A. Curtiss, P. C. Redfern, B. J. Smith, L. Radom, *J. Chem. Phys.* **1996**, *104*, 5148−5152.
[29] V. Barone, M. Cossi, J. Tomasi, *J. Chem. Phys.* **1997**, *107*, 3210−3221.
[30] J. Tomasi, M. Persico, *Chem. Rev.* **1994**, *94*, 2027−2094.
[31] N. Díaz, D. Suárez, T. L. Sordo, *Chem. Eur. J.* **1999**, *5*, 1045−1054.
[32] D. A. McQuarrie, *Statistical Mechanics*, Harper Collins Publishers, Inc., New York, **1976**.
[33] A. Warshel, *Computer Modelling of Chemical Reactions in Enzymes and Solutions*, John Wiley & Sons, Inc., New York, **1991**.
[34] P. A. Kollman, B. Kuhn, M. Peräkylä, *J. Phys. Chem. B* **2002**, *106*, 1537−1542.
[35] J. Hermans, L. Wang, *J. Am. Chem. Soc.* **1997**, *119*, 2707−2714.

Received July 7, 2003

  